Strongly Driven Frequency-Sweeping Events in Plasmas

R. G. L. Vann,[1] H. L. Berk,[2] and A. R. Soto-Chavez[2]
[1]Department of Physics, University of York, Heslington, York YO10 5DD, United Kingdom
[2]Institute for Fusion Studies, The University of Texas, Austin, Texas 78712, USA
(Received 23 February 2007; published 13 July 2007)

A generic model of a kinetic plasma formed from a source and sink is presented which without instability would form a strongly unstable state due to a single mode. Instead, the resulting wave-particle resonant interaction maintains the distribution near a marginally stable state through the continual production of fast frequency-sweeping modes that sweep unidirectionally (upward in our case) throughout the energy-inverted region of the distribution function. The energy of these modes can be channeled to the background plasma through wave dissipation and, in our particular example, one quarter of the injected energy is available to be channeled.

DOI: 10.1103/PhysRevLett.99.025003 PACS numbers: 52.40.Mj, 52.35.Qz, 52.55.Pi, 52.65.Ff

In this Letter, we explore a basic wave-particle interaction in a thermal plasma with a substantial energetic particle beam. In particular we consider a regime in which the beam is so strong that the dispersion relation for linear waves is qualitatively different to its form when beams are absent. This is relevant to the ITER tokamak, currently under construction, which is predicted [1] in some situations to be unstable to energetic particle modes (EPMs)—modes that do not exist in the absence of energetic particles. The kinetic beam of particles we study here is paradigmatic for how alpha particles can relax in a burning plasma. In our model plasma, continually frequency-sweeping (or ''chirping'') modes are generated spontaneously and we suggest that these modes might be an energy channeling mechanism [2,3] for transferring a significant fraction of energetic particle energy to the plasma.

If the energy density fraction of energetic particles (EPs) relative to the (stable) thermal plasma is small, then the mode frequency ω is not significantly affected by them (i.e. $\delta\omega \ll \omega$) and the growth rate γ (typically $|\gamma| \ll \omega$) is determined by EP-driven resonant instabilities. Such a scenario may be classified as ''perturbative'' [4]. Previous numerical studies for this case [5] identified bifurcations and frequency sweeping, similar to the analytic theory of Refs. [6,7]. If the energy density of the EPs is sufficiently large, EPMs are generated; experimental examples of such ''nonperturbative'' phenomena include the fishbone mode [8–10] and other shear Alfvénic-like activity [4,11–13]. In this Letter we present results of a generic plasma model with sufficiently strong injection to generate a nonperturbative response. Then spontaneously driven chirping modes arise which force the particle distribution to hover near a marginally stable state that is far from what would be observed in the absence of waves. As a result of the nonlinear particle interaction with the chirping modes, a significant fraction ($\sim$25% in our simulation) of the beam particle energy is transported to lower energies. In conventional quasilinear theory [14] a spectrum of fixed-frequency linear waves is needed to cause relaxation of the distribution function to a marginal state; in this Letter a single chirping mode causes relaxation to marginal stability.

Our generic plasma model uses electrostatic waves with a single particle species and includes terms that represent fast particle injection, extrinsic background field damping and an annihilation term that models collisions [15,16]. This is the simplest example one can consider when investigating the consequence of a discrete wave-particle interaction. Here we use it to illustrate what may happen in the more complex Alfvén wave-energetic particle interaction, where, despite the added complexity, one can show through the use of action-angle variables that a similar description governs the nonlinear dynamics [17]. The kinetic equation for the distribution function $f(x, v, t)$ satisfies the Vlasov equation modified by a model source term and collision operator:

$$\frac{\partial f}{\partial t} + v\frac{\partial f}{\partial x} + E\frac{\partial f}{\partial v} = \nu F_{\text{beam}} - \nu(f - F_{\text{th}}), \qquad (1)$$

where νF_{beam} represents the injected EP beam and F_{th} the thermal background. In the absence of waves (i.e., $E = 0$), this equation drives $f \rightarrow F_0 = F_{\text{th}} + F_{\text{beam}}$ at a rate ν. The electric field $E(x, t)$ is determined by a consistent electrostatic equation, except for an extrinsic damping term that is added to the basic equation:

$$\frac{\partial E}{\partial t} + \int v f dv - \int v f_0 dv = -\gamma_d E, \qquad (2)$$

where f_0 denotes the spatial mean of f: the third term in Eq. (2) ensures that the left-hand side of this equation is equivalent to the Poisson operator for an electrostatic wave. The right-hand side can be viewed as modeling dissipative processes that are not otherwise described by the kinetic equation governing the distribution f, and which we view as due to additional charge-neutral currents that respond to applied fields in a linear resistive manner. The time scale is normalized to the inverse plasma frequency $\omega_p^{-1} = \sqrt{m\varepsilon_0/nq^2}$. Spatial lengths are normalized to the Debye length, velocities to the thermal speed

$v_{\rm th} = \sqrt{k_B T/m}$, and E to $(m/q)v_{\rm th}\omega_p$, where m, q, T, and n are the species' mass, charge, temperature, and number density, respectively. For the simulation described in this Letter we take

$$(2\pi)^{1/2} F_{\rm th} = \eta \exp(-v^2/2), \tag{3}$$

$$(2\pi)^{1/2} F_{\rm beam} = [(1-\eta)/v_a]\exp[-(v-v_b)^2/2v_a^2], \tag{4}$$

where we choose $\eta = 0.5$, $v_a = 1.0$, $v_b = 6.0$, and $(\gamma_d, \nu) = (0.4, 2 \times 10^{-4})$. The spatial interval is periodic with period $L = 8\pi$. If $f = F_0$ the system is unstable ($\omega = 0.829 + 0.243i$) for a mode with the wavelength $L = 8\pi$, while it is linearly stable for the allowed shorter wavelengths (L/n, with $n \geq 2$).

The simulation is initialized with $f(x, v, t = 0) = F_{\rm th}(v)$ and $E(x, t = 0) = 0$. The system evolves at first by constitution of the beam at the injection rate ν: $f = F_{\rm th} + \alpha(t) F_{\rm beam}$ where $\alpha(t) = 1 - \exp(-\nu t)$. Once the beam density α exceeds the critical value $\alpha_{\rm crit} = 0.075$, the system becomes linearly unstable with respect to modes of wavelength L. The long time behavior of the system is shown in Fig. 1: the field undergoes repeated fast frequency-sweeping (chirping) events; the modes sweep predominantly upwards and have the form $\delta\omega \propto \delta t$, in contrast to the perturbative result for which there is a predominantly symmetric chirp produced with $\delta\omega \propto \pm\sqrt{\delta t}$ [6].

We now consider the snapshot of f_0 at $t = 9750$ shown in Fig. 2; this time is chosen because it is the time at which the structure shown in Fig. 5 (to be discussed later) achieves its maximum amplitude. The spatially averaged distribution $f_0(v)$ is shown as a solid line; the steady-state equilibrium solution distribution $F_0(v)$ is shown as a dotted line for comparison. The arrows indicate the phase velocity of modes excited in the plasma at that instant: these are calculated by taking a cross section through Fig. 1 and extracting the maxima, whose positions give the frequencies (which are transformed to velocities via $v = \omega/k$). We note that the energy difference between f_0 and F_0 is large and that the waves' phase velocities correspond to holes in f_0 whose velocities increase in time. In contrast to the previously reported perturbative case [5–7], the long time evolution of the distribution function is not a small perturbation about the state ($f = F_0$, $E = 0$).

A snapshot of the distribution function $f(x, v)$ at the same time $t = 9750$ is shown in Fig. 3. This Figure demonstrates the complexity of the dynamics. At least three islands are visible in this plot with phase velocities of 5.4, 3.5, and 6.6 (in order of size), corresponding to the density holes shown in Fig. 2. If we write $E = E_1 \cos(kx - \omega t + \Phi)$, then the trapping width in velocity space $\Delta v = 4\sqrt{E_1/k}$. Using $E_1 = 0.069$ from Fig. 5 gives a trapping width $\Delta v = 2.1$, which is about 40% less than what is observed. This is because the island is compressed in v on both sides by other trapping islands. (When there is no adjacent trapping region, the expression used for the island width is verified.)

These phase space structures sweep over a velocity space domain that is large compared to the instantaneous trapping width. This can be seen from Fig. 1 (using the relation phase velocity $v_\phi = \omega/k$). This large sweep enables a single phase space structure to extract much more energy from a broader band of energetic particles velocities than a single stationary mode. We expect that the continuously chirping distribution function will hover close to a relaxed distribution function that is at marginal stability (i.e., the distribution's most unstable mode is marginally stable), in much the same way that a multimode quasilinear system with sources and sinks would be close to marginal stability [18]. This motivates a study of the linear stability of a relaxed steady-state uniform distribution $F(v)$ [not $F_0(v)$]. The dispersion relation is $D(\omega, k) = 0$, where, for real ω and $k > 0$, and denoting the principal part by P,

$$\mathrm{Re}\, D(\omega, k) \equiv D_r(\omega, k) = k^2 - \mathrm{P}\int_{-\infty}^{+\infty} \frac{\frac{dF}{dv} dv}{v - \omega/k}, \tag{5}$$

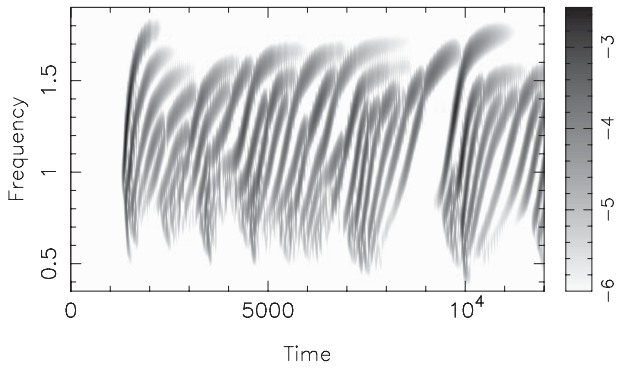

FIG. 1. Field mode spectrum $\tilde{E}_1(\omega, t)$ from generic model simulation exhibits nonperturbative frequency sweeping: $\delta\omega \propto \delta t$. The logarithmic gray scale has range [0.001, 0.08].

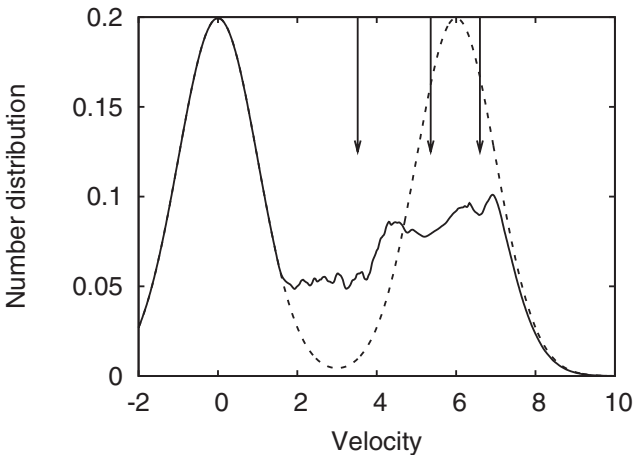

FIG. 2. A snapshot of $f_0(v)$ at $t = 9750$ (solid line) and $F_0(v)$ (dashed line). The arrows show the phase velocities of the modes present at this time, all of which are increasing.

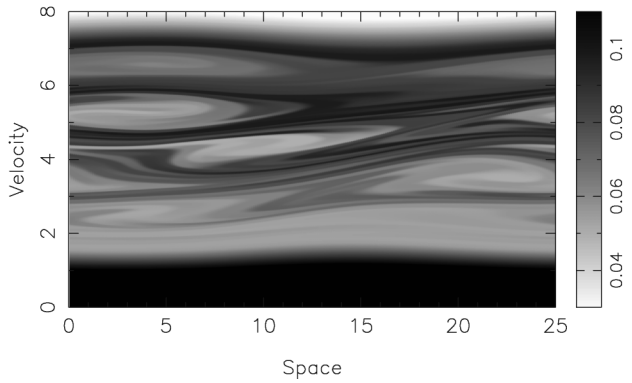

FIG. 3. A snapshot of $f(x, v)$ also at $t = 9750$. Several islands are visible in this plot; over time their phase velocities increase, corresponding to an increase in the frequency of the associated modes.

$$\mathrm{Im}\, D(\omega, k) \equiv D_i(\omega, k) = -\pi\left[\frac{dF}{dv} - \frac{\gamma_d k}{\pi v}\right]_{v=\omega/k}. \quad (6)$$

Returning to Fig. 2, we observe that there is a region in velocity $\mathcal{H} = [v: v_1 < v < v_2]$ over which the distribution function is maintained far from $F_0(v)$ by the sweeping of the phase space structures. Figure 4 shows that in this region the long time average $f_0(v)$ varies approximately linearly in velocity, while outside the region being swept, $f_0 \approx F_0$. To test the hypothesis that the system persists near marginal stability we construct a candidate distribution $F(v)$ that is marginally stable, varies linearly in velocity in the region where the distribution is strongly distorted, and continuously links to $F_0(v)$ outside the distorted region. We then compare $F(v)$ to the temporally averaged distribution observed in the simulation. Thus the conditions on F are: (a) $\int F(v)dv = 1$ (which can be shown to time asymptotically follow from the zeroth space and velocity moment of Eq. (1); (b) $F(v) = b(v - v_1) + F_0(v_1)$ if $v \in \mathcal{H}$ (b, v_1, and v_2 to be determined); (c) $F(v) = F_0(v)$ if $v \notin \mathcal{H}$; (d) $F(v)$ satisfy the marginal stability criterion. For our input parameters these conditions yield the solution $v_1 = 1.69$, $v_2 = 7.02$, $b = 0.0133$; the real part of the dispersion relation gives the phase velocity $v_\phi = 2.39$. The candidate distribution $F(v)$ is plotted in Fig. 4 and can be compared with the temporal average of f_0: $\bar{f}_0(v) = (t_2 - t_1)^{-1} \int_{t_1}^{t_2} f_0(v)dt$, which is also plotted. This distribution is independent of (t_1, t_2) in the limit that t_1 and $(t_2 - t_1)$ are large; for this plot we chose $t_1 = 5 \times 10^4$ and $t_2 = 10^5$. We note that $\bar{f}_0(v)$ and $F(v)$ are comparable, although the slope of the averaged distribution is somewhat less than the slope of the candidate distribution. This indicates that on average the system is slightly stable in linear theory to a nonperturbative mode. An analysis of the chirp onset condition for nonperturbative modes near marginal stability given in Ref. [19] indicates that the upward direction of the chirp is preferred for our instability. Furthermore, at the initial excitation of a marginally stable mode, the phase velocity is much closer to the minimum of $f_0(v)$ than its maximum. Consequently, the holes can move a large distance in increasing velocity, but any clumps that are formed cannot sweep very far before being subsumed by the thermal bulk. A magnification of Fig. 1 shows that many hole-clump pairs form, but the holes are short lived.

The theoretically calculated sweeping formula calculated in [6] and generalized in [17] shows that background dissipation forces the trapping region (which is locked to the mode frequency) to move in phase space to where the trapping structure has lower energy (note that phase space holes have lower energy where particles have higher energy) and thereby energy is released to balance the dissipation [20]. This model then predicts $\delta\omega \propto t^{1/2}$ when the linear dielectric function $D_r(\omega)$, in the electrostatic charge relation $iD_r(\omega)kE(\omega) = \rho_{\mathrm{hole}}(\omega)$ [here $E(\omega)$ is the Fourier-transformed electric field and ρ_{hole} is the hole charge density], is expanded linearly about the frequency of its marginal stability point ω_0, i.e., where $D_r(\omega_0) = 0$ so that $D_r(\omega) \approx (\omega - \omega_0)\frac{\partial D_r(\omega_0)}{\partial \omega}$. This theoretical model for sweeping has been recalculated for the nonperturbative regime keeping the exact form for $D_r(\omega)$ (where ω is real) with otherwise the same assumptions as Ref. [6]. The equilibrium distribution chosen is $F(v)$ as calculated above. The resulting theoretical calculations for phase velocity and amplitude are plotted with the results from the simulation in Fig. 5. The simulation quantities are for a single structure that has been isolated by taking the maxima for each point in time from Fig. 1 and then searching for connected structures with lifetime $\tau > 500$. The only fitting parameter is the time offset. The comparison between theory and simulation is good; deviations are likely to result from interactions between adjacent structures in the simulation (which we already know affects the island width) and mixing of trapped and passing particles, neither of which is included in the current theoretical modeling.

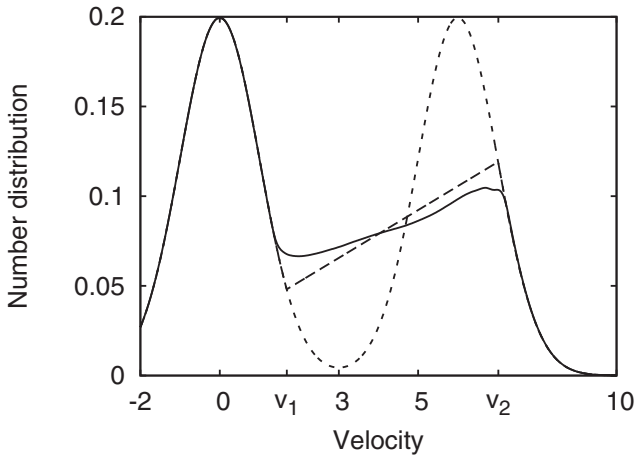

FIG. 4. The long time average $\bar{f}_0(v)$ (the solid line) is observed to be approximately linear across the wide region (v_1, v_2) where it differs from $F_0(v)$ (the dotted line). The dashed line shows the marginal stability distribution $F(v)$ predicted by the theory described in the text.

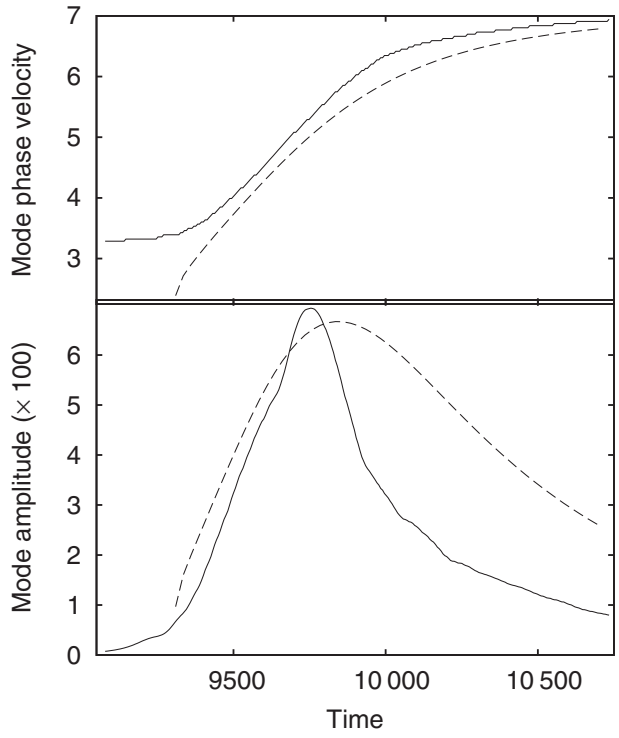

FIG. 5. Analysis of a single structure. Simulation (solid line) and theory (dashed line) show good agreement for both phase velocity and mode amplitude.

The maintenance of a marginal state by chirping modes suggests a variant of energy channeling first proposed by Fisch and Rax [2]. From Eqs. (1) and (2), the rate of change of stored energy is found to be

$$\frac{d\mathcal{E}}{dt} = \nu L \int_{-\infty}^{+\infty} \frac{1}{2} v^2 (F_0 - f_0) dv - \gamma_d \int_0^L E^2 dx. \quad (7)$$

We note that the system eventually hovers about marginal stability where the stored energy remains roughly constant so that on average the left-hand side of Eq. (7) vanishes. Thus, time averaged energy transfer takes the form

$$\nu L \int_{-\infty}^{+\infty} \frac{1}{2} v^2 F_0 dv = \nu L \int_{-\infty}^{+\infty} \frac{1}{2} v^2 f_0 dv + \gamma_d \int_0^L E^2 dx. \quad (8)$$

This expression shows that the input power on the left-hand side from EP injection is balanced by both the classical output power mechanism of EPs (in our modeling it is due to the particle annihilation) and the power extracted by dissipation of the excited waves that chirp predominantly upward in frequency. The ratio of the first to second terms on the right-hand side is found to be 3:1. In a physical system both energetic particle energy extracted by collisions (modeled here by annihilation) and wave power extracted by dissipation would be absorbed by the background plasma. Provided the energy being extracted through both channels heats the plasma and energetic particles are not lost to the walls, the background plasma will be heated at the rate at which beam power is supplied. In our model a significant part of the heating of the plasma background is through the chirping wave channel. As a result, the actual near-steady-state energetic particle distribution function established is 25% less energetic than the one that is predicted from the classical transport process (here annihilation) alone. Such a reduction of stored energy could prevent other energetic particle instabilities being excited. If one can establish this type of benign chirping mechanism in a burning fusion plasma experiment, where the energetic alpha particles transfer comparable or more power through the wave heating channel than through the electron drag channel, a higher fusion power output could be achieved [21].

The authors thank B. N. Breizman, M. P. Gryaznevich, and S. E. Sharapov for useful discussions. This work was funded in part by the UK EPSRC and U. S. DOE Grant No. DE-FG02-04ER54742. Computing facilities were provided by the Centre for Scientific Computing at the University of Warwick with support from JREI Grant No. JR00WASTEQ, and at the University of York with support from EPSRC Grant No. R47769.

[1] G. Vlad *et al.*, Nucl. Fusion **46**, 1 (2006).
[2] N. J. Fisch and J.-M. Rax, Phys. Rev. Lett. **69**, 612 (1992).
[3] H. L. Berk and B. N. Breizman, Comments Plasma Phys. Control. Fusion **17**, 129 (1996).
[4] M. P. Gryaznevich and S. E. Sharapov, Nucl. Fusion **46**, S942 (2006).
[5] R. G. L. Vann, R. O. Dendy, and M. P. Gryaznevich, Phys. Plasmas **12**, 032501 (2005).
[6] H. L. Berk, B. N. Breizman, and N. V. Petviashvili, Phys. Lett. A **234**, 213 (1997); **238**, 408(E) (1998).
[7] H. L. Berk, B. N. Breizman, and M. Pekker, Phys. Rev. Lett. **76**, 1256 (1996).
[8] K. McGuire *et al.*, Phys. Rev. Lett. **50**, 891 (1983).
[9] L. Chen, R. B. White, and M. N. Rosenbluth, Phys. Rev. Lett. **52**, 1122 (1984).
[10] E. Fredrickson, L. Chen, and R. White, Nucl. Fusion **43**, 1258 (2003).
[11] S. Bernabei *et al.*, Nucl. Fusion **41**, 513 (2001).
[12] F. Zonca and L. Chen, Phys. Plasmas **3**, 323 (1996).
[13] L. Chen, Phys. Plasmas **1**, 1519 (1994).
[14] N. N. Gorelenkov, H. L. Berk, and R. V. Budny, Nucl. Fusion **45**, 226 (2005).
[15] H. L. Berk and B. N. Breizman, Phys. Fluids B **2**, 2226 (1990); **2**, 2235 (1990); **2**, 2246 (1990).
[16] R. G. L. Vann *et al.*, Phys. Plasmas **10**, 623 (2003).
[17] H. L. Berk *et al.*, Phys. Plasmas **6**, 3102 (1999).
[18] H. L. Berk and B. N. Breizman, in *Joint Varenna-Lausanne International Workshop on Theory of Fusion Plasmas, Varenna, Italy, 1998*, edited by J. W. Connor, E. Sindoni, and J. Vaclavik (SIF, Bologna, 1998), p. 283.
[19] B. N. Breizman *et al.*, Phys. Plasmas **4**, 1559 (1997).
[20] K. V. Roberts, Comput. Phys. Commun. **3**, 14 (1972).
[21] S. D. Pinches *et al.*, Plasma Phys. Controlled Fusion **46**, B187 (2004).